Journal of Informatics Education and Research
ISSN: 1526-4726
Vol 5 Issue 2 (2025)

Morphometric analysis of coracoid process and glenoid width -3D CT

***Mani Pratap Singh M.SC. Research fellow[1], Amit Bisht Assistant professor[2]**
[1]Department of Radiology and Imaging Techniques, college of paramedical science, Teerthanker Mahaveer University, Moradabad.
[2]Department of Radiology and Imaging Techniques, college of paramedical science, Teerthanker Mahaveer University, Moradabad.
Corresponding Email id : manipratap713@gmail.com

Abstract
Aim-The purpose of this study was to use 3D CT to examine the morphometric parameters in the glenoid width and coracoid process in the UP western population.
Objective - Using morphometric parameter shows difference according to age and gender related differences in UP western population.
Method- A total of 72 patients, age ranges between 20 to 75 years old, and the samples were collected from the Department of Radiology, Teerthanker Mahaveer Hospital and Research Centre Moradabad, Uttar Pradesh. In this study, we measured the morphometric parameters of the coracoid region and glenoid width using three-dimensional computed tomography with volume rendering software for image visualisation. Computed tomography united imaging 160 slice machine. Data was collected from the osirix platform and make 3D image with thin slices then various parameters were measured from Radiant Dicom viewer. And performed a statistical analysis on all those collected evaluates of the glenoid width and coracoid process which was taken by me during my research project.
Result-The study indicates that all variables are associated with both gender and age. All parameters exhibited positive correlations with one another. The Pearson correlation coefficient ("r") was employed to ascertain the relationship between the different characteristics of the coracoid process and glenoid width. The G.W (mm), coracoid length from tip to base (mm), C.TIP H (mm), C.TIP Width (mm), midpoint W. (mm), distance from midpoint to base (mm), and midpoint H (mm) exhibited a positive correlation ($p < 0.05$) with one another.
Conculsion-A comparative analysis of the process of coracoid and glenoid width demonstrated a statistically significant difference ($p < 0.05$) in the following metrics: glenoid width (mm), length of the coracoid from tip to base(mm), coracoid tip height (mm), coracoid tip width (mm), midpoint width (mm), distance from midpoint to base (mm), and midpoint height (mm), categorised by age groups utilising One Way ANOVA. The independent sample 't' test is utilised to compare the coracoid process and glenoid width, demonstrating a significant difference ($p < 0.05$) in the following measurements between males and females: glenoid width (mm), length of the coracoid from tip to base(mm), coracoid tip height (mm), coracoid tip width (mm), midpoint width (mm), distance from midpoint to base (mm), and midpoint height (mm). The Pearson correlation coefficient (“r”) was utilised to examine the link between the various attributes of the coracoid process and glenoid breadth. The G.W (mm), length of the coracoid from tip to base(mm), Coracoid tip height (mm), Coracoid tip width (mm), midpoint width (mm), Distance from midpoint to base (mm), and midpoint height (mm) demonstrated a statistically significant positive connection ($p < 0.05$) among themselves.

Keywords: Blood supply, Coracoid process, Glenoid width, IPD, Morphometric analysis, OPD , 3D Reconstruction

1. Introduction

The coracoid process is a hook-shaped bony structure that arises anterolaterally from the superior aspect of the scapular neck. Surgeons frequently designate the coracoid process as the "lighthouse of the shoulder." The Latin term for shoulder denotes the scapula, a slender bone located on the posterolateral aspect of the thoracic cavity. The scapula possesses three processes, two surfaces, three borders, and three angles. With the glenoid cavity, the outer or glenoid (Greek shallow form) angle is large. (1), (4)

The triangular spine divides the convex dorsal surface into the supraspinous and infraspinous fossae. The coastal region is utilised by the convex thoracic wall and the concave subscapular fossa. From the inferior angle below to the glenoid cavity above, the thickest lateral border is seen. (1)

The costal surface, or subscapular fossa, is concave and orientated anteriorly and medially. It is characterised by three longitudinal ridges. The lateral boundary is an additional substantial ridge that is contiguous to it. When the arm is elevated overhead, this elongated segment of bone functions as a lever for the serratus anterior muscle. (1), (6)

The spine attaches to the posterior aspect of the scapula, dividing it into a tiny supraspinous fossa and a greater infraspinous fossa. Two fossae are connected by the Spino glenoid notch, located laterally to the spinal root.

The coracoid process is directed anteriorly and slightly laterally (derived from the Greek term meaning "resembling a crow's beak"). It resembles a distorted digit. This type of epiphysis is primitive.

The superior border is slender and more abbreviated. The base of the coracoid process is next to the suprascapular notch. The lateral margin is robust. The infra glenoid tubercle is observed at the apex. The medial edge is slender. It descends from the superior angle to the inferior angle. (1), (3)

The trapezius encompasses the superior angle. The latissimus dorsi encompasses the inferior angle. When the arm is removed, it progresses around the torso. The glenoid cavity, orientated anteriorly, laterally, and slightly superiorly, is situated within the expansive lateral or glenoid angle. (6)

The spine, identified as the triangular bone plate termed the spinous process, with three edges and two surfaces. It partitions the dorsal aspect of the scapula into the supraspinous and infraspinous fossae. The posterior edge is referred to as the spinal crest. The lips on the crest are both superior and inferior. The acromion consists of a facet for the clavicle, two superior and inferior surfaces, and two lateral and medial borders.

The multipennate subscapularis develops from the medial section of the remaining two-thirds in the subscapular fossa. The supraspinatus arises from the medial a second-third of the supraspinous fossa, located on the upper surface of the scapula. The infraspinatus arises from the medial two-thirds of the infraspinous fossa located on the inferior surface of the scapula.

The deltoid muscle arises from the lateral margin of the acromion and the inferior edge of the spinal crest. The fibres of the acromion resemble several coins. The long head of the biceps brachii originates from the supraglenoid tubercle, whereas the short head arises from the lateral aspect of the coracoid process. The medial border of the costal surface provides support for the serratus anterior muscle. One digitation runs from the superior angle to the spinal base, two digitations originate from the inferior angle, and five digitations emerge from the medial boundary. The supraglenoid tubercle is the origin of the long head of the biceps brachii, whereas the lateral portion of the coracoid process serves as the origin for the short head. The coracobrachialis originates from the medial aspect of the coracoid process tip. The pectoralis

minor connects to the superior surface and medial border of the coracoid process. The infra glenoid tubercle is the origin of the long head of the triceps brachii. The teres minor originates from the upper two-thirds of the rough band on the dorsal side near the lateral border. The teres major emerges from the lowest segment of the rough strip on the dorsal aspect of the lateral border. From the superior angle to the spine's root, the levator scapulae insert along the dorsal part of the medial border. The rhomboid minor is situated opposite the origin of the spine along the medial border (dorsal aspect). The rhomboid major is located between the inferior angle and the spine's root, on the dorsal side of the medial border. The inferior belly of the omohyoid originates from the superior border near the suprascapular notch. The periphery of the glenoid cavity represents the interface between the shoulder joint capsule and the glenoid labrum. (5)
The acromioclavicular joint capsule is attached to the border of the facet on the medial edge of the acromion. The coracoacromial ligament is affixed to the lateral edge of the coracoid process and the medial aspect of the acromion process apex. The coracohumeral ligament is affixed to the base of the coracoid process. The coracoclavicular ligament is linked to the coracoid process. (1), (4)
The glenohumeral joint functions as a diarthrodial, multiaxial joint, despite being a ball-and-socket joint. The glenohumeral joint, the primary joint of the shoulder girdle, connects the humeral head to the glenoid cavity of the scapula. (2), (3) The glenohumeral joint is the most mobile joint in the human body. Excessive movement across many planes in the body is facilitated by static and dynamic stabilising structures, rendering the joint more susceptible to instability incidents. (7), (2)
The proximal humerus and the scapular glenoid interact intricately and dynamically at the glenohumeral joint, which is a ball and socket joint. In particular, the head of the humerus joins the glenoid chamber, or fossa, of the scapula. (2), (8) Articular cartilage lines both of their articulating surfaces. The glenoid cavity, a shallow osseous element, is structurally deepened by the glenoid labarum, a fibrocartilaginous ring that surrounds the vault's osseous perimeter. The superior aspect of the labarum connects it to the biceps brachii tendon. (2), (5). (9)

2. Material Methodology

A total of 72 patients, age ranges between 20 to 75 years old, and the samples were collected from the Department of Radiology, Teerthanker Mahaveer Hospital and Research Centre Moradabad, Uttar Pradesh. In this study, we measured the morphometric parameters of the coracoid region and glenoid width using three-dimensional computed tomography with volume rendering software for image visualisation. Computed tomography united imaging 160 slice machine. parameters include such as -

- **Glenoid width**
- **Coracoid length tip to base**
- **Coracoid tip height**
- **Coracoid tip width**
- **Coracoid mid-point height**
- **Coracoid from midpoint to tip base**
- **Coracoid midpoint width**

Data was collected from the osirix platform and make 3D image with thin slices then various parameters were measured from Radiant Dicom viewer. The patient who are sent to the department of radio diagnosis for shoulder joint CT examination. A source of data Both IPD and OPD patients are included who meet all the inclusion and exclusion criteria. Include patient

Included patient age between 20 to 75 years, patient include who is no pathology in coracoid process and glenoid cavity. Excluded patients Exclude patients whose age above 75 years Traumatic patients are excluded. This is prospective and cross-sectional based. duration of this research 1 year.

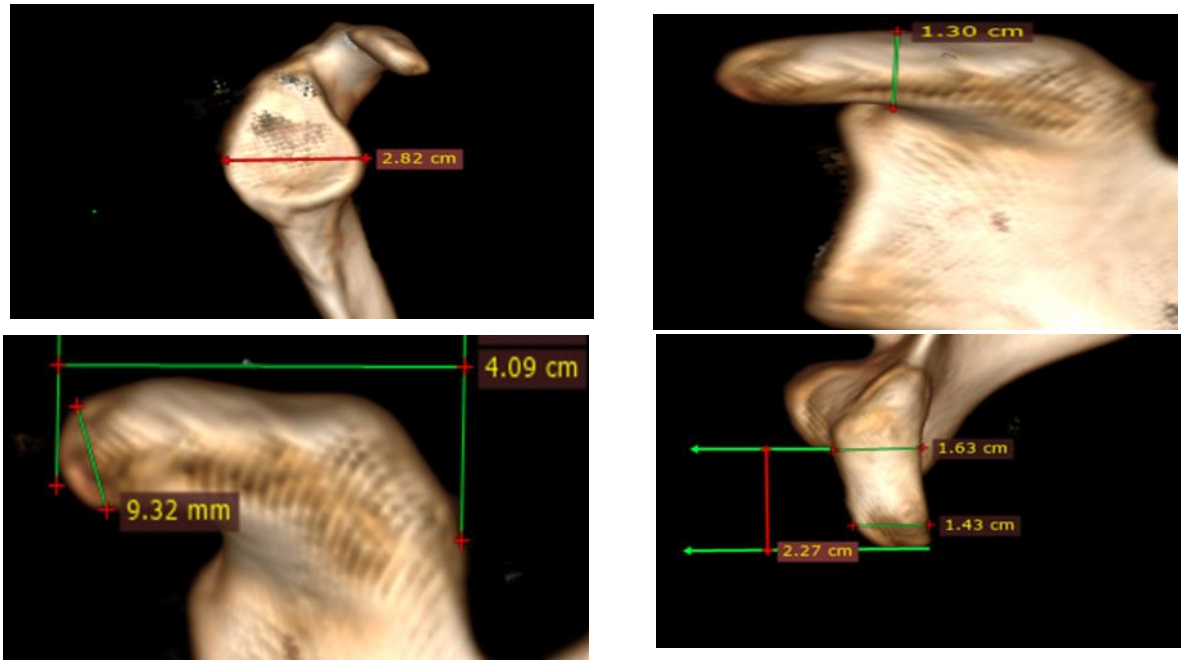

Figure 1.1 – Measurement of 3D view coracoid process and glenoid width

3. Results

3D reconstruction computerized Tomographic Scans (CT scans) of 72 patients (Males- 46 and Females-26) various morphometric measurement is used for examined the coracoid process and glenoid width. Included parameters AGE, GW, CLTB, CTH, CTW, MPW, DMB, MPH. The Mean value and SD value 43.39±14.53 ,25±2.52 ,42.93±4.23 ,8.61±1.14 ,12.89±1.57 ,15.11±1.70 ,20.73±2.50 ,13.69±1.64. The independent sample t-test compared the process of the coracoid and glenoid width based on gender, revealing significant differences ($p < 0.05$) in glenoid width and coracoid process measurements (GW, CLTB, CTH, CTW, MPW, DMB, MPH) between males and females. A one-way ANOVA was employed to examine the coracoid process and glenoid breadth, utilizing GW, CLTB, CTH, CTW, MPW, DMB, and MPH, categorized by age group. A statistically significant difference ($p< 0.05$) was seen in the coracoid process and glenoid breadth across the age groups. The study indicates that all variables are associated with both gender and age. All parameters exhibited positive correlations with one another. The Pearson correlation coefficient ("r") was employed to ascertain the relationship between the different characteristics of the coracoid process and glenoid width. The G.W (mm), coracoid length from tip to base (mm), C.TIP H (mm), C.TIP Width (mm), midpoint W. (mm), distance from midpoint to base (mm), and midpoint H (mm) exhibited a positive correlation ($p < 0.05$) with one another. The collected data were summarized by using the Descriptive Statistics: frequency, percentage; mean and S.D. To compare the coracoid process and glenoid width: G.W (mm), coracoid length tip to base (mm), C.TIP H (mm), C.TIP Width (mm), midpoint W.(mm), distance from midpoint to base (mm) as well as the midpoint H

(mm); between males and females; the independent sample "t" test was used. The One-way ANOVA was used to compare the coracoid process and glenoid width; according to age groups. The Post hoc analysis, Tukey test was used for the multiple comparisons of coracoid process and glenoid width according to the age groups: 20-35 vs. 36-55; 20-35 vs. 56-71; and 36-55 vs. 56-71 years. Also, the independent sample "t" test was used to compare the coracoid process and glenoid width according to gender within the age groups. To compare the coracoid process and glenoid width according to age group within gender; the One-way ANOVA was used. The Pearson correlation coefficient ("r") was used to find the relation between the various parameters of coracoid process and glenoid width. The p value < 0.05 was considered as significant. Data were analyzed by using the SPSS software (SPSS Inc.; Chicago, IL) version 29.0.10.

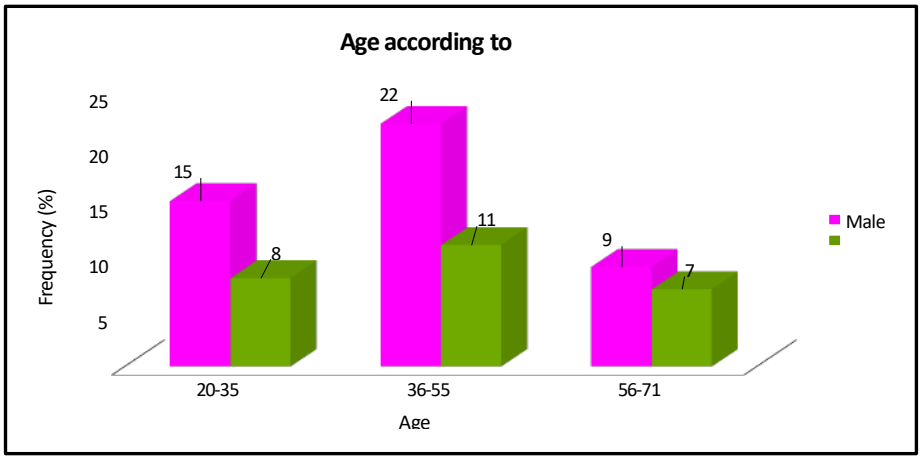

Graph 1.1. Represents the Age according to gender

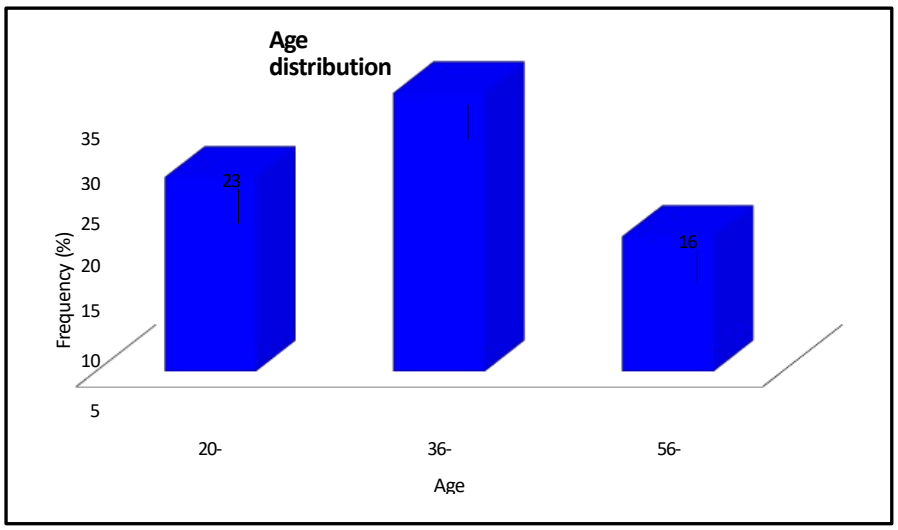

Graph 1.2 Represent the Age distribution

Table 1.1 Comparison of the coracoid process and glenoid width according to age groups

		Mean	S.D.	"F"	p value
G.W (mm)	20-35	24.96	2.75	6.73	0.002*
	36-55	25.67	2.27		
	56-71	22.84	2.74		

Coracoid length tip to base (mm)	20-35	42.06	3.99	11.45	< 0.001*
	36-55	43.65	3.78		
	56-71	37.44	5.48		
C.TIP H (mm)	20-35	8.72	1.18	8.35	0.001*
	36-55	8.72	0.95		
	56-71	7.50	1.08		
C.TIP Width (mm)	20-35	13.07	1.81	6.15	0.003*
	36-55	12.88	1.36		
	56-71	14.45	1.36		
Midpoint W.(mm)	20-35	15.00	1.52	9.30	< 0.001*
	36-55	15.02	1.73		
	56-71	17.09	1.90		
Distance from midpoint to base (mm)	20-35	20.17	2.72	5.34	0.007*
	36-55	21.02	2.37		
	56-71	22.66	1.60		
Midpoint H (mm)	20-35	13.79	1.51	5.03	0.009*
	36-55	13.52	1.66		
	56-71	14.97	1.16		

("F" = One-way ANOVA; * Significant)

		Mean	S.D.	"t"	p value
G.W (mm)	Male	26.21	2.37	5.15	< 0.001*
	Female	23.48	1.71		
Coracoid length tip to base (mm)	Male	44.40	4.17	4.41	< 0.001*
	Female	40.32	2.92		
C.TIP H (mm)	Male	8.86	1.26	2.57	0.012*
	Female	8.17	0.73		
C.TIP Width (mm)	Male	13.43	1.52	4.34	< 0.001*
	Female	11.93	1.18		
Midpoint W.(mm)	Male	15.72	1.73	4.60	< 0.001*
	Female	14.02	0.97		
Distance from midpoint to base (mm)	Male	21.36	2.17	3.00	0.004*
	Female	19.62	2.69		
Midpoint H (mm)	Male	14.32	1.59	4.95	< 0.001*
	Female	12.59	1.06		

("t" = Independent sample "t" test; * Significant)

4. Discussion

This study compared from others research's, **Yaofei Jia et.al. (2020) China,** using morphometric parameter 3D reconstruction computerized tomographic scans (CT scans) of 84 patients (Males-55 and females -29) using this parameter to measure the coracoid process

and glenoid width. Included parameters AGE, GW, CLTB, CTH, CTW, MPW, DMB, MPH. the Mean and SD value, 41.63 ± 12.06 ,27.86 ± 2.69, 41.60 ± 4.04, 9.05 ± 1.83,13.09 ± 2.06, 20.80 ± 2.02, 11.12 ± 1.97, 14.59 ± 2.07. In this study no significant difference in among aged group is observed (P > 0.0). (6) **Jean-Pierre du Plessis et.al. (2020) at Cape Town, South Africa,** Using morphometric parameters from 3D reconstruction computerized tomographic scans, measurements were taken from One hundred consecutive patients (fifty male and fifty female) regarding coracoid width (16.5±1.4 mm vs. 14.7±1.4 mm) and height (13.6±1.6 mm vs. 10.5±1.5 mm). The anteroposterior glenoid dimension (25.3±2.9 mm vs. 23.2±2.4 mm) exhibited a gender difference of 1.8 mm and 3.1 mm, respectively. This study revealed a statistically significant difference ($p<0.05$) in coracoid height between the gender groups. All morphometric analyses demonstrated a statistically significant gender difference ($p<0.05$), except for coracoid length. (5) **Sandra Mathews et.al. (2017) at Zurich,** A multi-modal cadaveric study utilising morphological parameters and 3D reconstruction from computerised tomographic scans (CT scans) assessed glenoid measurements, incorporating isolated scapulae from 18 male and female donors (average age 84 years, range 60–98 years). Included parameter Glenoid height, Glenoid width. The mean and standard deviation for males is glenoid height 39.5 mm ± 3.5 and width 30.3 mm ± 3.3; for females, glenoid height is 34.8 mm ± 2.2 and width 26.2 mm ± 1.6. There exists significant sexual dimorphism ($p < 0.001$) in the average glenoid height of 36.6 mm ± 3.6 and width of 27.8 mm ± 3.1.(10) **In our study, at UP Western Moradabad** 3D reconstruction computerized Tomographic Scans (CT scans) of 72 patients (Males- 46 and Females-26) various morphometric measurement is used for examined the coracoid process and glenoid width. Included parameters AGE, GW, CLTB, CTH, CTW, MPW, DMB, MPH. The Mean value and SD value 43.39±14.53 ,25±2.52 ,42.93±4.23 ,8.61±1.14 ,12.89±1.57 ,15.11±1.70 ,20.73±2.50 ,13.69±1.64. The independent sample t-test compared the process of the coracoid and glenoid width based on gender, revealing significant differences ($p < 0.05$) in glenoid width and coracoid process measurements (GW, CLTB, CTH, CTW, MPW, DMB, MPH) between males and females. A one-way ANOVA was employed to examine the coracoid process and glenoid breadth, utilizing GW, CLTB, CTH, CTW, MPW, DMB, and MPH, categorized by age group. A statistically significant difference ($p< 0.05$) was seen in the coracoid process and glenoid breadth across the age groups. The study indicates that all variables are associated with both gender and age. All parameters exhibited positive correlations with one another. The Pearson correlation coefficient ("r") was employed to ascertain the relationship between the different characteristics of the coracoid process and glenoid width. The G.W (mm), coracoid length from tip to base (mm), C.TIP H (mm), C.TIP Width (mm), midpoint W. (mm), distance from midpoint to base (mm), and midpoint H (mm) exhibited a positive correlation ($p < 0.05$) with one another.

Table 1.3 – Comparing various studies morphometric parameter

	Yaofei Jia et.al			**OUR STUDY**		
Parameter	**AGE**	**MEAN**	**S.D.**	**AGE**	**MEAN**	**S.D.**
G.W (mm)	20-30	27.67	2.90	20-35	24.96	2.75
	31-40	27.30	2.43	36-55	25.67	2.27
	41-50	27.82	2.52	56-71	22.84	2.74
	51-60	28.36	2.88	-	-	-

Coracoid length tip to base (mm)	20-30	41.96	3.91	20-35	42.06	3.99
	31-40	40.92	4.40	36-55	43.65	3.78
	41-50	41.96	3.47	56-71	37.44	5.48
	51-60	41.96	4.60	-	-	-
C.TIPH (mm)	20-30	9.08	1.72	20-35	8.72	1.18
	31-40	8.52	1.99	36-55	8.72	0.95
	41-50	8.76	1.39	56-71	7.50	1.08
	51-60	9.60	2.12	-	-	-
C.TIP Width (mm)	20-30	12.90	1.69	20-35	13.07	1.81
	31-40	12.99	2.38	36-55	12.88	1.36
	41-50	12.75	1.88	56-71	14.45	1.36
	51-60	13.64	2.32	-	-	-
Midpoint W. (mm)	20-30	14.40	2.03	20-35	15.00	1.52
	31-40	14.15	2.14	36-55	15.02	1.73
	41-50	14.52	1.99	56-71	17.09	1.90
	51-60	15.07	2.17	-	-	-
Distance from midpoint to base (mm)	20-30	20.98	1.95	20-35	20.17	2.72
	31-40	20.46	2.20	36-55	21.02	2.37
	41-50	20.67	1.74	56-71	22.66	1.60
	51-60	20.98	2.30	-	-	-
Midpoint H (mm)	20-30	11.64	2.22	20-35	13.79	1.51
	31-40	10.55	1.89	36-55	13.52	1.66
	41-50	10.89	1.62	56-71	14.97	1.16
	51-60	11.23	2.10	-	-	-

5. Conclusion

A comparative analysis of the process of coracoid and glenoid width demonstrated a statistically significant difference ($p < 0.05$) in the following metrics: glenoid width (mm), length of the coracoid from tip to base(mm), coracoid tip height (mm), coracoid tip width (mm), midpoint width (mm), distance from midpoint to base (mm), and midpoint height (mm), categorised by age groups utilising One Way ANOVA. The independent sample 't' test is utilised to compare the coracoid process and glenoid width, demonstrating a significant difference ($p < 0.05$) in the following measurements between males and females: glenoid width (mm), length of the coracoid from tip to base(mm), coracoid tip height (mm), coracoid tip width (mm), midpoint width (mm), distance from midpoint to base (mm), and midpoint height (mm). The Pearson correlation coefficient ("r") was utilised to examine the link between the various attributes of the coracoid process and glenoid breadth. The G.W (mm), length of the coracoid
from tip to base(mm), Coracoid tip height (mm), Coracoid tip width (mm), midpoint width (mm), Distance from midpoint to base (mm), and midpoint height (mm) demonstrated a statistically significant positive connection ($p < 0.05$) among themselves.

Future perspectives

- Helps in morphology structure of Age and gender differences of coracoid process and glenoid width.
- In coracoid osteotomy.

- It helps to the surgeons in the evaluation of coracoid process transfer.

Limitationsss

- The study conducted using small sample size.
- Included only non-traumatic and non-pathology patient.
- Included only 20–75-year aged patient.

References

1. BD Chaurasia's Human Anatomy, Volume 1 - Upper Limb Thorax, 6th Edition.
2. Anatomy, Shoulder and Upper Limb, Glenohumeral Joint | Treatment & Management | Point of Care.
3. Mangasah H, Aminata IW. Three-dimensional morphometric analysis of glenoid in the Indonesian population and its clinical significance. Journal of Orthopaedics. 2023 Mar; 37:27–33.
4. Raviprasanna K, Chaitra B, Benjamin W, Mangasuli V. Coracoid Process of Scapula: Morphometric Analysis in South Indian Population. IJARS [Internet]. 2022 [cited 2025 Apr 21]; Available from: https://www.ijars.net/article_fulltext.aspx?issn=0973-709x&year=2022&month=April&volume=11&issue=2&page=AO06%20-%20AO10&id=2756
5. Du Plessis JP, Dey R, Dachs R, De Wet TJ, Trevor T, Carrara H, et al. A gender-based comparison of coracoid and glenoid anatomy: CT analysis and discussion of potential impact on the Latarjet procedure. Journal of Shoulder and Elbow Surgery. 2021 Jul;30(7):1503–10.
6. Jia Y, He N, Liu J, Zhang G, Zhou J, Wu D, et al. Morphometric analysis of the coracoid process and glenoid width: a 3D-CT study. J Orthop Surg Res. 2020 Dec;15(1):69.
7. Morphometric Analysis of Coracoid Process in Adult Human Scapula in Eastern Odisha Population. IJFMT [Internet]. 2020 Oct 7 [cited 2025 Apr 21]; Available from: http://medicopublication.com/index.php/ijfmt/article/view/13022
8. Ozel O, Hudek R, Abdrabou MS, Werner BS, Gohlke F. The implications of the glenoid angles and rotator cuff status in patients with osteoarthritis undergoing shoulder arthroplasty. BMC Musculoskelet Disord. 2020 Dec;21(1):668.
9. Matsuki K, Sugaya H, Hoshika S, Ueda Y, Takahashi N, Tokai M, et al. Three-dimensional measurement of glenoid dimensions and orientations. Journal of Orthopaedic Science. 2019 Jul;24(4):624–30.
10. Mathews S, Burkhard M, Serrano N, Link K, Häusler M, Frater N, et al. Glenoid morphology in light of anatomical and reverse total shoulder arthroplasty: a dissection- and 3D- CT-based study in male and female body donors. BMC Musculoskelet Disord. 2017 Dec;18(1):9.